



HAL
open science

Rare-Earth-Doped Y₂SiO₅ Crystal Directly Bonded on Glass for Efficient Optical Quantum Technologies Platform

Anne Talneau, Sacha Welinski, Alban Ferrier

► **To cite this version:**

Anne Talneau, Sacha Welinski, Alban Ferrier. Rare-Earth-Doped Y₂SiO₅ Crystal Directly Bonded on Glass for Efficient Optical Quantum Technologies Platform. *physica status solidi (a)*, 2024, Phys. Status Solidi A 2024, 2300718, 10.1002/pssa.202300718 . hal-04475234

HAL Id: hal-04475234

<https://hal.science/hal-04475234>

Submitted on 23 Feb 2024

HAL is a multi-disciplinary open access archive for the deposit and dissemination of scientific research documents, whether they are published or not. The documents may come from teaching and research institutions in France or abroad, or from public or private research centers.

L'archive ouverte pluridisciplinaire **HAL**, est destinée au dépôt et à la diffusion de documents scientifiques de niveau recherche, publiés ou non, émanant des établissements d'enseignement et de recherche français ou étrangers, des laboratoires publics ou privés.

Rare-Earth-Doped Y_2SiO_5 Crystal Directly Bonded on Glass for Efficient Optical Quantum Technologies Platform

Anne Talneau,* Sacha Welinski, and Alban Ferrier

For high-efficiency optical quantum technology platforms, bonding rare-earth doped crystals on glass are of great interest, enabling the enhancement of the optical guided mode interaction with the active rare-earth ions. Optical coherence lifetimes and stable operation are operated at very low temperature (3–4 K). Bonding should be preferably performed without adding any intermediate sticking layer in order not to hamper the optical mode distribution and propagation. Directly bonded Y_2SiO_5 crystal on a borosilicate glass is shown and the bonding mechanisms are discussed.

1. Introduction

Quantum memories are a key element for optical quantum communications. Quantum memories based on rare-earth-doped crystals offer long optical coherence lifetimes and stable operation at very low temperature (3–4 K).^[1–3] Current devices suffer from a storage reduced efficiency related to the weak interaction between the light and the active ions. Bonding the REC on a lower-refractive-index glass substrate and etching waveguides on the REC bonded membrane would allow building a photonic integrated platform where the increased interaction with the active ions will translate into better efficiency. Moreover, this scalable and versatile integrated photonic platform will allow developing new compact building blocks with extended

functionalities such as fiber-integrated quantum memories or microwave-to-optics photon transducers.

Yttrium orthosilicate crystal Y_2SiO_5 -doped Er^{3+} (Er:YSO) has been chosen due to its optimal low noise properties, allowing very large coherence lifetime.^[3–5]

Direct molecular bonding is the best bonding choice for elaborating a photonic platform, leading to the maximal interaction of the guided mode with the REC material and compatible with the low-temperature operation. On the contrary,

if a bonding agent would be included as an interstitial layer at the interface, this thicker interface will translate in a reduced interaction of the guided mode with the REC and the included bonding agent could degrade the operating mechanism at very low temperature.

Direct molecular bonding is performed at a temperature chosen in order to reconstruct chemical bonds at the interface of the two materials. YSO being a very stable crystal, the main concern for choosing the bonding temperature will be driven by the D263 glass material. The glass transition temperature T_g is one of the main parameters that describes the structural behavior of a glass material. We will consider T_g for the discussion of the results proposed in this article.

2. Bonded Materials

The yttrium orthosilicate Y_2SiO_5 -doped Er^{3+} (Er:YSO) crystal is a very stable crystal elaborated from the melt by the Czochralski method,^[5] at temperature above 1200 °C.

The glass material choice has been dictated by the thermal behavior compatibility of both materials: one consideration is the low-temperature operation of the hybrid platform in the 3–4 K range and the second one is the bonding procedure requiring annealing for covalent bonds generation. For the best behavior in these 2 situations, both materials should have a coefficient of thermal expansion (CTE) as close as possible one from the other. The YSO CTE being $= 7.4 \times 10^{-6} \text{ °C}^{-1}$, we have chosen the D 263 T borosilicate glass from Schott, which has a CTE (D263) $= 7.2 \times 10^{-6} \text{ °C}^{-1}$,^[6] very close to the CTE of YSO.


The D263 T is a borosilicate glass. Compared to pure silica glass having a very high glass transformation temperature T_g in the range of 1700 °C, adding boron to silica glass, generating a borosilicate glass enables reducing its T_g ; the larger the B_2O_3 concentration the larger the T_g reduction.^[7,8] The D263 borosilicate glass includes as its main compositors SiO_2 , B_2O_3 , and Na_2O , B and Si being the network formers and the alkaline element Na

A. Talneau
CNRS, C2N Centre de Nanosciences et de Nanotechnologies
CNRS C2N
10 Bd Thomas Gobert, Palaiseau F-91120, France
E-mail: anne.talneau@c2n.upsaclay.fr

S. Welinski
Thales Group
Research & Technology
1 Av. Augustin Fresnel, F-91120 Palaiseau, France

A. Ferrier
Chimie ParisTech
PSL University
CNRS
Institut de Recherche de Chimie Paris
F-75005 Paris, France

A. Ferrier
Faculté des Sciences et Ingénierie
Sorbonne Université
UFR 933, F-75005 Paris, France

 The ORCID identification number(s) for the author(s) of this article can be found under <https://doi.org/10.1002/pssa.202300718>.

DOI: 10.1002/pssa.202300718

being a network modifier. No glass composition is provided by Schott in the D263 datasheet.^[6] Related to the provided T_g value, $T_g = 557^\circ\text{C}$.^[6] We tentatively infer its composition to be close to the following proportions: $\text{SiO}_2 \approx 60\%$, $\text{B}_2\text{O}_3 \approx 20\%$, and the soda proportion Na_2O being the remaining $\approx 20\%$ part if we consider only these three main components.^[9–11] The temperature-dependent behavior of borosilicate glass is complex in the presence of soda content, affecting the Bore coordination.^[12–14] When the temperature is increased, remaining below T_g , the glassy network is rearranged, mainly related to the transformation of triangular bore BO_3 to tetrahedra bore BO_4 , thus modifying the glass viscosity and generating nonbridging oxygen NBO. These NBO are electrically compensated by Na^+ ions. This NBO generation has been evidenced by Raman analysis^[9,12,13] in Na-containing borates and borosilicates. This viscosity modification is intended to occur when the temperature approaches very closely T_g .

3. Bonding Results

Figure 1 shows a strioscopic imaging of the entire YSO piece bonded on D263, evidencing the distribution of optical index variation over a large part of the bonded material area. **Figure 2** shows an optical microscope image of the upper-left corner of YSO and the glass in the area close to YSO. The optical index variation could be related to bubbles, which are located within the glass below the YSO and close to the YSO borders. The bubbles are intended to be within the glass material since a mechanical profilometer measurement on the glass surface close to the YSO shows a glass flat surface.

In order to confirm this observation, we cleaved/cut the bonded stack and made a scanning electron microscope (SEM) image of the cross-section plan. **Figure 3** shows the

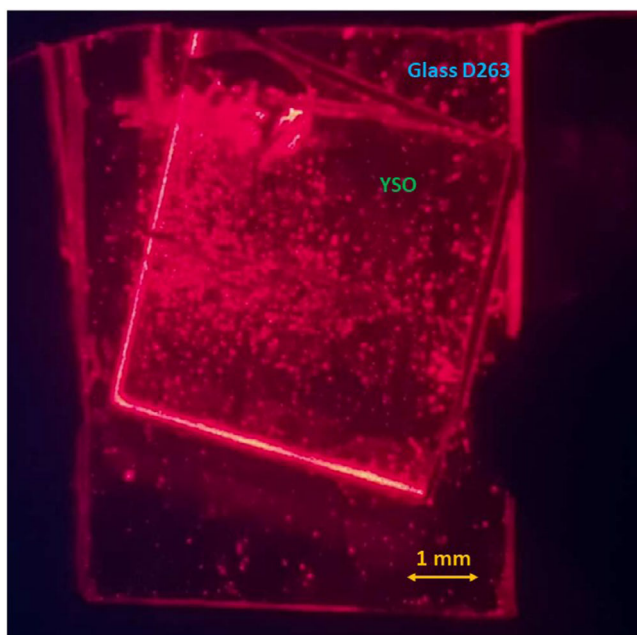


Figure 1. Strioscopic imaging of the whole bonded YSO material, evidencing the distribution of optical index variation.

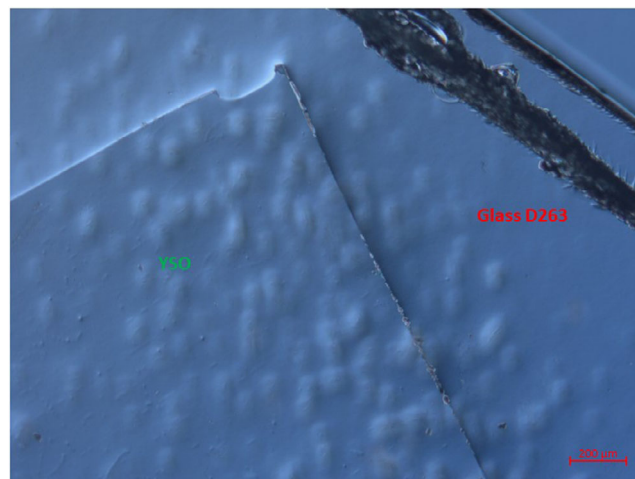


Figure 2. Optical microscope image of YSO bonded on D263 Schott glass. Bonding is performed at 520°C for 3 h, under low pressure (2 MPa).

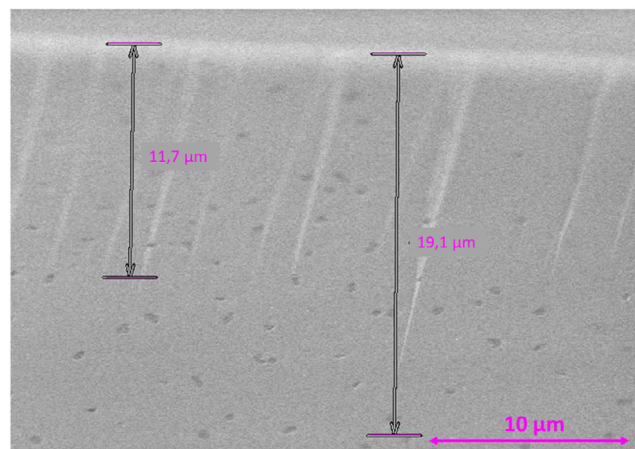


Figure 3. Bubbles distribution within the glass material, below the YSO. The hybrid YSO//glass interface appears on top, as a white fuzzy line.

SEM distribution of the bubbles below YSO from the hybrid interface visible on top as a fuzzy white line, down to $\approx 20\ \mu\text{m}$ within the glass. Zooming is performed on **Figure 4**, showing three bubbles, the typical size of these bubbles being 600–800 nm extension. Bubbles are not so present very close to the hybrid interface. Their distribution starts to be denser at $\approx 10\ \mu\text{m}$ down in the glass, they are not anymore present when reaching down to $\approx 100\ \mu\text{m}$.

Within the SEM equipment, we have performed an energy-dispersive X-ray spectroscopy (EDX) analysis following the cross-section plan, starting in the YSO 250 μm far from the interface, then moving to the hybrid interface, crossing the interface, and following in the glass down to 100 μm . The atomic percentage of several elements has been recorded in **Figure 5**. EDX measurements are performed at 10 keV, the probe size being $1\ \mu\text{m}^3$. The bore element is not visible, due to the too low sensitivity of the detector.

These measurements evidence a strong Carbone contamination close to both surfaces, due to the clean-room environment.

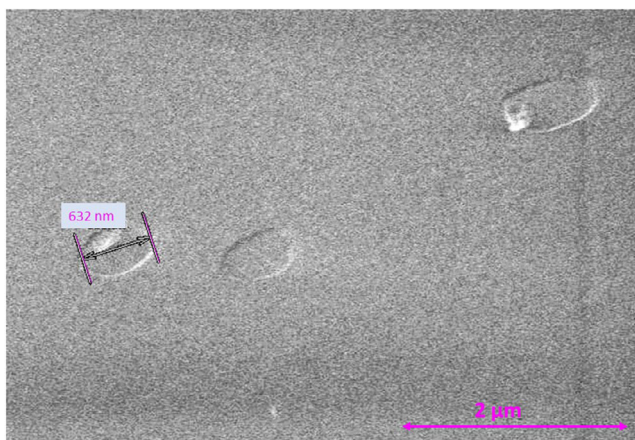


Figure 4. Details of bubbles, in the $\approx 20 \mu\text{m}$ region down from the interface.

Following the elements of interest for the bonding procedure, we see that K element is measured, indicating that K_2O is probably one network modifier included in the D263 glass. Both Na and K atomic percentages are not measured close to the interface, which is the glass surface, probably due to a specific glass surface treatment during the fabrication process. The Y element distribution evidences an increase of its atomic percentage close to the interface and even a small transfer through the interface. The YSO surface having been capped by a 20 nm-thick SiO_2 layer prior bonding, this SiO_2 layer could have contributed during annealing to migration of Y element close to the surface, thus depleting the region behind the surface. This proposed mechanism is a first attempt that has to be confirmed by further investigation and also has to be analyzed related to the probe size, which is $\approx 1 \mu\text{m}^3$.

4. Proposed Mechanisms and Discussion

Bubbles are observed due to their imprint in the glass. This is possible since the annealing is performed at 520°C , a temperature which is quite close to the T_g of the glass. In the viscosity

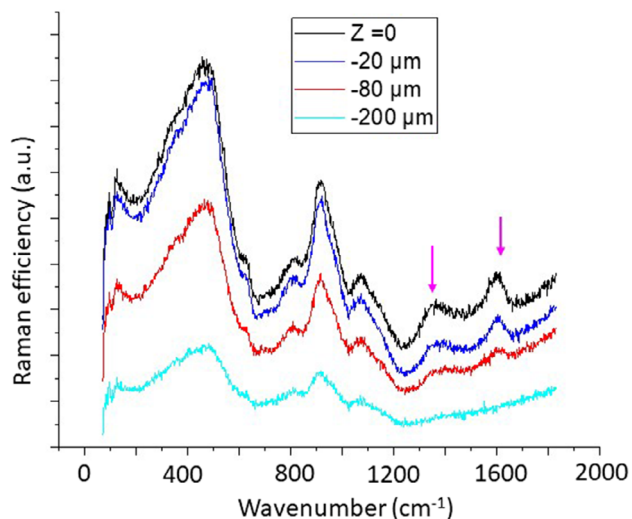


Figure 6. Raman efficiency versus wavenumber, measured on the glass close to the YSO border, at the glass surface and for three different focusing planes within the glass.

variation having a log shape close to T_g , this shows that the glass viscosity is affected. Related to this viscosity modification, a contribution of non-bridging oxygen (NBO) generation could be considered. To check such a possible NBO generation, we performed Raman spectroscopy measurements within the glass, close to the YSO border, in order to be in the zone where the glass is affected by the bonding mechanism, as bubbles' signature shows, but without adding the YSO Raman lines in order to facilitate the spectra understanding. A Renishaw μ Raman equipped with a confocal source @ $\lambda = 532 \text{ nm}$ is used. We performed different measurements, the results are shown in **Figure 6**, focusing from the surface $z = 0$ (black curve) down in the glass to $20 \mu\text{m}$ (blue curve), to $80 \mu\text{m}$ (red curve), and finally to $200 \mu\text{m}$ (cyan curve). We measured up to the $1400\text{--}1600 \text{ cm}^{-1}$ wavenumber domain, where the signature of NBO generation could be expected if any.^[9,10] Two small peaks can be identified related to these specific signatures, the most important efficiency observed at the glass surface.

| Element | Glass | | | | | Interface | YSO | | | |
|---------|-------------------------|------------------------|------------------------|------------------------|-----------------------|---------------------|----------------------|----------------------|-----------------------|--|
| | Glass 100 μm | Glass 50 μm | Glass 20 μm | Glass 10 μm | Glass 5 μm | YSO 5 μm | YSO 20 μm | YSO 50 μm | YSO 250 μm | |
| C | | | 21,38 | 63,18 | 54,32 | 19,58 | 59,60 | 50,30 | 9,62 | |
| O | 71,40 | 62,71 | 49,85 | 32,70 | 38,11 | 60,06 | 39,14 | 46,99 | 72,65 | |
| Na | 5,34 | 5,32 | 2,78 | | | | | | | |
| Si | 20,71 | 28,72 | 22,10 | 4,11 | 5,90 | 7,47 | 1,22 | 1,54 | 5,87 | |
| K | 1,96 | 3,25 | 2,09 | | | | | | | |
| Y | | | | | 1,62 | 12,85 | | 1,17 | 1,97 | |

Figure 5. EDX atomic percentages of the measured elements, following the cross section of the YSO//glass-bonded stack.

Even though these peaks are observed in the wavenumber domain where the NBO signature is expected, they are very small; the annealing temperature being 520 °C, it is too far from the T_g to consider that NBO generation could be the driving mechanism involved.

The dissociation of Na_2O is the main mechanism to be considered, Na_2O being well known to be dissociated at low temperature. The dissociation of Na_2O is the driving mechanism of anodic bonding performed at 200 °C.^[15] We then proposed that, related to the annealing temperature being 520 °C, and the applied pressure being 2 MPa, Na_2O is dissociated, generating O which condensates in O₂ bubbles that are trapped in the glass network whose viscosity is only slightly affected at that temperature. The pressure applied has a decisive contribution, even though its value is small.^[16,17] Reducing the applied pressure is under investigation, the preliminary experiments without pressure at all, leading to no bonding.

Related to the very strong mechanical behavior of the hybrid YSO//glass stack allowing cleaving, we infer that covalent bonds have been reconstructed at the interface. Mechanical measurement of the bonding energy would be out of scope of this article. Si-O-Si bonds reconstruction is fully described and mastered in the silicon semiconductor industry for bonding large-scale silicon wafers.^[18] The YSO crystal being capped by a thin SiO_2 layer, when annealed after bonded to glass, we propose that the same Si-O-Si reconstruction of covalent bonds is the mechanism which is the most likely to occur in order to produce the very strong interface. Here, we have implemented the optimized oxide preparation with ozone that has been developed for electrical transport through a hybrid InP//Si interface.^[19]

5. Conclusion

Bonding the rare-earth doped crystals YSO on a borosilicate glass substrate of lower optical index is intended for building a photonic integrated platform where efficient interaction between light and active ions of Er^{3+} -doped YSO will be possible. Such a larger interaction will lead to increased efficiency. Bonding preparation and conditions have been investigated, producing oxygen bubbles within the glass due to Na_2O dissociation. Reducing or ideally suppressing these bubbles in the borosilicate glass close to the interface is under investigation, since this material alteration will hinder the expected performances due to the related propagation losses generated.

6. Experimental Section

Bonding was here investigated without adding any intermediate sticking material. This direct molecular bonding procedure has the advantage of including no additional layer that could hamper the low-temperature (4 K) operation. This approach translates in covalent bond reconstruction at the interface. Considering the two materials involved YSO and the borosilicate glass, Si—O—Si bonds appear as the best candidates to be the reconstructed bonds. YSO being a very stable crystalline network, it is highly unlikely that an Si from the crystalline YSO network could be engaged in a Si—O—Si bond reconstruction. We chose to deposit a thin SiO_2 amorphous layer on top of the YSO crystal surface in order to have at our disposal Si atoms that could be engaged in Si—O—Si bond reconstruction when annealing was performed at a temperature that should remain

below the D263 glass $T_g = 557$ °C. This amorphous silica layer had a thickness in the 5–20 nm.

We investigated here bonding operating conditions in order to produce a bonded interface without alteration of both materials. Indeed, any alteration of YSO or glass at the interface should translate in propagation losses for the guided mode, thus hindering the expected performances.

The operating conditions are here presented. Both surfaces have to be clean, planar, and show a very low roughness; its root mean square was calculated as the mean square average of the profile height deviations from the mean line being below 1 nm.^[20] Related to the D263 T_g being 557 °C, bonding temperatures were investigated in the 500–550 °C range with the aim of modifying the glass network as little as possible. Bonding was operated under vacuum with a very low charge pressure, in the 1–2 MPa range. This pressure should only ensure contact between the two surfaces.

Both surfaces were cleaned in ultrasonic isopropanol bath for 5 min. A thin amorphous SiO_2 layer was deposited on the YSO surface by plasma-enhanced chemical vapor deposition at 280 °C. Such a layer was expected to allow a smooth transition between the crystalline YSO structure and the amorphous glass structure. This SiO_2 layer was activated by ozone for 5 min before being put down on the glass surface. Several glass surface preparations and bonding conditions were investigated. As for the glass surface preparation, we investigated surface cleaning with the Caro acid and with the SC1 preparation @70 °C^[21] each one alone, and also associated. For both acids, the duration was 10 min, followed by 10 min rinsing. As for the bonding conditions, we investigated temperatures in the 500–530 °C range, with a 10 °C step.

We presented here the successful bonded stack obtained when the glass surface was prepared with Caro acid followed by SC1 solution. The bonding temperature was set to 520 °C for 3 h, operated under vacuum 10^{-2} mTorr, with a small 2 MPa pressure. Samples were ≈ 1 cm², YSO being smaller than the underlying D263 glass.

Acknowledgements

This work was undertaken within the C2N micro nanotechnologies platforms and partly supported by the RENATECH network and the General Council of Essonne. The authors thank Pr. D.R. Neuville from IPGP, Paris, for very fruitful discussions.

Conflict of Interest

The authors declare no conflict of interest.

Data Availability Statement

The data that support the findings of this study are available from the corresponding author upon reasonable request.

Keywords

direct bonding, optical glass platforms, rare-earth doped crystals

Received: September 15, 2023

Revised: December 8, 2023

Published online:

[1] A. M. Dibos, M. Raha, C. M. Phenicie, J. D. Thompson, *Phys. Rev. Lett.* **2018**, *120*, 243601.

[2] S. Welinsli, A. Tiranov, M. Businger, A. Ferrier, M. Afzelius, P. Goldner, *Phys. Rev. X* **2020**, *10*, 031060.

- [3] P. Goldner, A. Ferrier, O. Guillot-Noël, in *Handbook on the Physics and Chemistry of Rare Earths* (Eds: J.-C. G. Bünzli, V. K. Pecharsky), Elsevier, Amsterdam **2015**, pp. 1–78.
- [4] B. Merkel, A. Ulanowski, A. Reiserer, *Phys. Rev. X* **2020**, *10*, 041025.
- [5] G. Wolfowicz, H. Maier-Flaig, R. Marino, A. Ferrier, H. Vezin, J. J. L. Morton, P. Goldner, *Phys. Rev. Lett.* **2015**, *114*, 170503.
- [6] D263 Schott datasheet, <https://www.schott.com/en-id/products/d-263-p1000318/downloads>.
- [7] E. Le Bourhis, *Glass, Mechanics and Technology*, Wiley-VCH, GmbH & CO. KGaA, Weinheim **2008**, ISBN 978-3-527-31549-9.
- [8] D. R. Neuville, L. Cornier, D. Caurant, L. Montagne, *From Glass to Crystal*, EDP Sciences, Paris France **2017**.
- [9] D. Manara, A. Grandjean, D. R. Neuville, *Am. Mineral.* **2009**, *94*, 777.
- [10] D. Manara, A. Grandjean, D. R. Neuville, *J. Non-Cryst. Solids* **2009**, *355*, 2528.
- [11] M. Lenoir, A. Grandjean, Y. Linard, B. Cochain, D. R. Neuville, *Chem. Geol.* **2008**, *256*, 316.
- [12] T. Edwards, T. Endo, J. H. Walton, S. Sen, *Sci. Res. Rep.* **2014**, *345*, 1027.
- [13] O. L. G. Alderman, C. J. Benmore, A. Lin, A. Tamalonis, J. K. R. Weber, *J. Am. Ceram. Soc.* **2018**, <https://doi.org/10.1111/jace.15529>.
- [14] E. F. Medvedev, N. I. Min'ko, *IOP Conf. Series: Mater. Sci. Eng.* **2018**, *327*, 032038.
- [15] K. B. Albaugh, *J. Electrochem. Soc.* **1991**, *138*, 3089.
- [16] G. Molnar, P. Ganster, A. Tanguy, E. Barthel, *Acta Mater.* **2016**, *111*, 129.
- [17] G. Molnar, P. Ganster, A. Tanguy, *Phys. Rev. E* **2017**, *95*, 043001.
- [18] F. Fournel, C. Martin-Cocher, D. Radisson, V. Larrey, E. Beche, C. Morales, P. A. Delean, F. Rieutord, H. Moriceau, *ECS J. Solid State Sci. Technol.* **2015**, *4*, P124.
- [19] A. Talneau, G. Beaudoin, G. Patriarche, F. Ducroquet, *Phys. Status Solidi A* **2021**, *218*, 2000317.
- [20] Q.-Y. Tong, U. Gösele, *Semiconductor Wafer Bonding*, Wiley, New York **1998**.
- [21] M. Chemla, D. Levy, S. Petitdidier, F. Rouelle, S. Zanna, *Electrochemistry* **2004**, *72*, 238.